33rd Annual International Conference of the IEEE EMBS
Boston, Massachusetts USA, August 30 - September 3, 2011

3-D Modeling of Nitric Oxide Emission and Vasodilation Induced by CA3 Hippocampal Neurons

Alireza Nejati and Charles P. Unsworth, *Member IEEE*

***Abstract*— The modeling of the spread, diffusion, and decay of chemicals in the brain is a complex problem that is made difficult by the fact that the structures that produce chemicals (synapses etc.) may be very small in comparison to their radii of chemical influence. In this article, we concentrate on modeling a simple instance of this problem; that of a proficiently diffusing molecule that may cause changes in smooth muscle contractions over relatively large areas.**

An optimized diffusion system was developed to study the diffusion of neuronal nitric oxide. Our diffusion system allows us to model the spread of nitric oxide from all areas of neurons, including the soma and dendritic processes. In addition, our system allows us to model tiny diffusing structures without sacrificing large-scale granularity. To study the effect of NO-producing neurons on vasodilation, we simulate systems of 1 and 2 neurons. We show that it is possible for nitric oxide emitted from neurons to be involved in regulating blood flow.

I. Introduction

This work is focused at studying the effects of small and highly diffusive gaseous molecules. The clearest biological candidate for such a molecule would ostensibly be nitric oxide (NO). For the purposes of this study, instead of trying to capture the dynamics of a gaseous neurotransmitter in a general way (as has been done previously by many authors [7]), we instead focus on the peculiar properties of NO. Thus we model the production, diffusion, absorption, and decay of NO as accurately as required for our purposes.

II. Nitric oxide and the central nervous system

Nitric oxide is one of the few gaseous molecules known to be involved in signaling in the human body. In the last few decades it has emerged that NO plays the role of a neurotransmitter in the brain [6][3]. In the nervous system, only neurons have the ability to secrete nitric oxide, as nitric oxide synthase (NOS) occurs in neurons alone [1].

In the body, NO is primarily formed by nitric oxide synthase (NOS) enzymes. Ca^{2+} ions form a complex with calmodulin which binds with NOS to catalyze the synthesis of NO. Thus, the levels of NO in the brain are dependent upon Ca^{2+} levels.

The question of whether NO can directly (i.e. not through vasodilation and other indirect mechanisms) influence short-term neural activity is not one that has yet been answered with confidence. The fact that cGMP produced through NO can bind to cGMP-gated channels in the retina [10] opens up the possibility that NO might cause changes in membrane channel permeability in the central nervous system. However, a wide range of studies have indicated that NO does not directly affect neurons in this way [4]. It is possible that whether NO directly influences neurons or not, depends on the precise local conditions and cell types, explaining the apparent inconsistency between studies. Indeed, the precise local conditions have been shown to influence NO modulation behavior [6]. A good review of the literature is given in both [6] and [4].

III. Vasodilation

Vasodilation refers to the relaxation of the smooth muscle lining of blood vessel walls. The role of NO as a vasodilator is well-known [2]. It is conceivable that there might be mechanisms for neurons to release NO when higher nutrient levels are required [8]. Recent work seems to strengthen the hypothesis that one of the most important functions of NO in the brain is to draw more blood flow to regions of high synaptic activity [3]. It has been implied that it is this production of NO that causes the increased oxygen levels that are detected in blood-oxygen level dependent (BOLD) fMRI analyses.

There are many mechanisms that cause this dilatory relaxation; in this article we focus on the nitrovasodilator pathway i.e. the pathway mediated by cGMP. Contraction of muscles results from the interaction of myosin and actin proteins in muscles. cGMP regulates MLCP via activation of cGMP-association protein kinase (PKG) and MLCP cleaves phosphate groups from myosin light chain (MLC) proteins. This results in the inability of actin filaments to contract.

It has previously been mentioned that NO catalyzes the production of cGMP. The exact process through which this occurs involves several steps. NO binds with soluble guanylate cyclase (sGC) to form a set of complexes.

The base form of sGC is E_b; this binds with NO to form a six-coordinate (6c) complex, which may then decay to the 5c complex which is fully active [13]. The E_{5c} complex may then catalyze the production of cGMP from GTP. In order to quantify the effect of NO on cGMP production, we have the following set of coupled differential equations:

$$\frac{\mathrm{d}E_b}{\mathrm{d}t} = -k_1 E_b[\mathrm{NO}] + k_{-1}E_{6c} + K_4[\mathrm{cGMP}]^m E_{5c}$$
$$\frac{\mathrm{d}E_{6c}}{\mathrm{d}t} = k_1 E_b[\mathrm{NO}] - k_{-1}E_{6c} - k_2 E_{6c} - k_3 E_{6c}[\mathrm{NO}]$$
$$\frac{\mathrm{d}E_{5c}}{\mathrm{d}t} = k_3 E_{6c}[\mathrm{NO}] + k_2 E_{6c} - K_4[\mathrm{cGMP}]^m E_{5c}$$

A. Nejati is a PhD student in the Department of Engineering Science, University of Auckland, Auckland 1010, New Zealand. (phone: +64-9-373-7599 ext 87490; fax: +64-9-373-7468; email: alireza.n.j@gmail.com)

C. P. Unsworth is a Senior Lecturer in the Department of Engineering Science, The University of Auckland, Auckland 1010, New Zealand. email: c.unsworth@auckland.ac.nz

978-1-4244-4122-8/11/$26.00 ©2011 IEEE

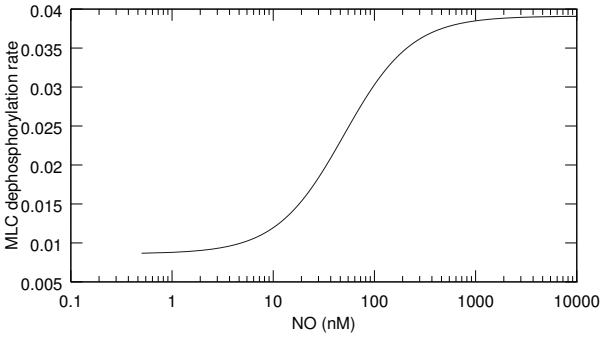

Fig. 1. NO causes vasodilation. Plotted is the steady-state solution of the relationship between the myosin light chain dephosphorylation rate (k_{mlcp}, see text) and NO concentration.

$$\frac{\mathrm{d}[\mathrm{cGMP}]}{\mathrm{d}t} = V_{max,sGC}E_{5c} - \frac{k_{\mathrm{pde}}[\mathrm{cGMP}]^2}{K_{\mathrm{m,pde}} + [\mathrm{cGMP}]} \quad (1)$$

Where E_b is equal to $[E_b]/[E_o]$, where $[E_o]$ is the total concentration of all forms of sGC (and likewise for E_{5c} and E_{6c}). Then, in order to quantify the effect of cGMP on MLC phosphorylation, we have the following equations:

$$R_{\mathrm{cGMP,mlcp}} = \frac{[\mathrm{cGMP}]^2}{[\mathrm{cGMP}]^2 + (5.5)^2}$$
$$k_{\mathrm{mlcp}} = k^{\mathrm{b}}_{\mathrm{mlcp}} + k^{\mathrm{c}}_{\mathrm{mlcp}} R_{\mathrm{cGMP,mlcp}}$$

Where k_{mlcp} is the rate of MLC dephosphorylation. A steady-state solution may be found. The steady-state solution is plotted in figure 1. A full discussion of this model, including the values of the constants, as well as the assumptions that were made, may be found in [13].

IV. NO DIFFUSION

We modeled the spread of NO according to the diffusion equation [12]:

$$\frac{\partial C}{\partial t} = D\nabla^2 C - \lambda C \quad (2)$$

Where $C(\mathbf{r}, x)$ is the concentration, D is the diffusion coefficient and λ is the decay constant. Determining λ is comparatively easy as there is no biological breakdown mechanism for NO [12]. NO only decays by oxidation, through interaction with various oxide and super-oxide molecules. The half-life of NO in nervous tissue has been estimated at being on the order of seconds (specifically, around 2 seconds [4]), dependent on the type of tissue and local conditions. Methods employing porphyrinic microsensors have estimated the diffusion coefficient of NO in the aorta wall of rats to be 3.3×10^{-5} cm^2/s [9].

We model the NO emission from the neuron as being at a constant rate per unit volume of neuronal cytoplasm. The production rate of NO in neuronal cytoplasm varies depending on the type of neuron, local conditions, etc. There have been a wide range of values reported in the literature. In [12], the production from a synapse with a radius of 1 μm is given as 2.1×10^{-17} mol/$\mu\mathrm{m}^3$s, while in [14] it is justified at 8.4×10^{-20} mol/$\mu\mathrm{m}^3$s based on parameters from the literature. We simulate the diffusion at various levels of NO production.

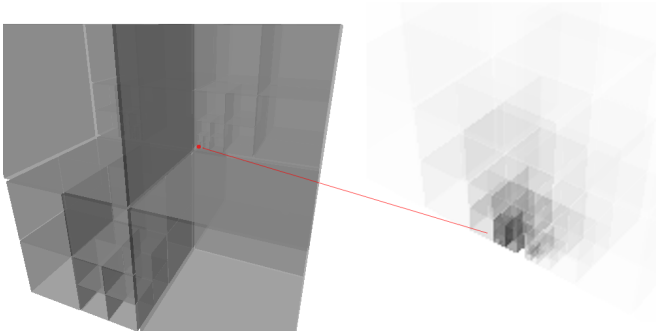

Fig. 2. Octree-based diffusion modeling. Left: a typical octree. Right: The same octree, with one of smallest cubes in the upper-middle of the cube being used as a diffusion source. The opacity of each sub-cube is proportional to the concentration.

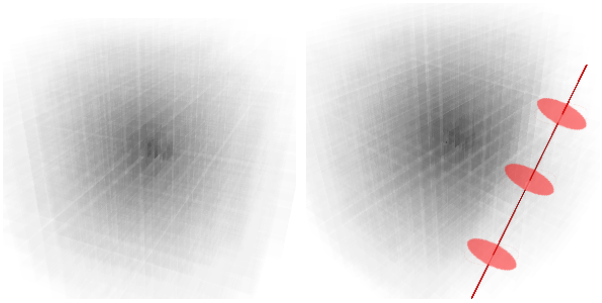

Fig. 3. Fine-grained diffusion octree. Right: inclusion of a cylindrical area where the diffusion parameters are different. The center and 3 cross sections of the area are highlighted in red. This structure could correspond to, for example, a blood vessel.

For numerical NO diffusion simulation, a wide variety of models were considered. We found few models that met our demands for modeling a dynamically-changing diffusion environment. We settled on using an octree-based system.

The octree model allows NO sources to be of any size, and for each source diffusion can be stopped and started at any time. The diffusion system is capable of simulating diffusive volumes with inhomogeneous parameters (for example, different diffusion constants for the inside and outside of a blood vessel). In Figure 2, a simple example of the method is illustrated. An example octree is shown, and it is then shown being used for diffusion simulation, with the concentration in the outside space being a constant 0. The subdivision is coarse, resulting in highly discontinuous 'jumps' of concentration. A finer subdivision may be seen in figure 3.

A. Diffusion from 3D neural model

For the purposes of our study we recognized the need to use a 3-dimensional neuron model since NO is emitted from all segments of the neuron. In addition, to facilitate future work in studying the synchronization properties in large ensembles of neurons, accurate signal propagation delays between neurons must be taken into account. Signal delays

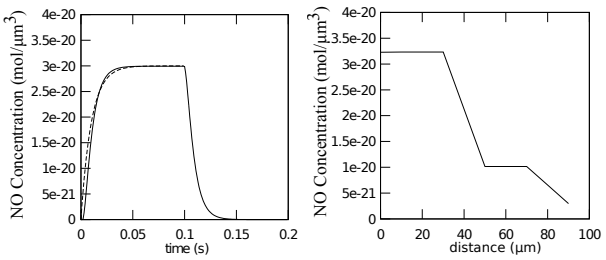

Fig. 4. Left: Modeling of an NO source where production is continuous from $t = 0$ to $t = 100$ ms and then stops. The concentration is shown at a distance of 100 μm (solid line). The theoretical curve is the dashed line. According to theory, the curve may be approximated by an exponential one (dashed curve). For the theoretical curve, we do not model NO fall time due to cutoff at 100 ms. Right: NO attentuation with distance from source.

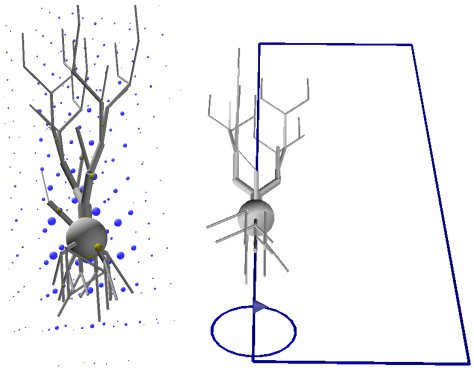

Fig. 5. CA3 hippocampal neuron with NO diffusion. Spheres represent NO concentration after 50 ms of diffusion. NO was sampled at a regular grid; however, it is important to note that the diffusion model is not a regular grid. Right: Visualizing the NO field around single neurons: a virtual plane is swept around the z-axis of the neuron and the average concentration is taken at each point on the plane (see figure 6).

may only be accurately modeled by approximating the 3-dimensional structure of neural networks.

The compartmental neuron model that we used was the model of a hippocampal CA3 neuron given in [11]. The neuron model includes an axon base but does not include an axon due to the fact that the axons of CA3 neurons often extend to relatively large distances before branching out. The model may be seen visualized in figure 5, along with NO diffusion simulation. The radius of the soma is about 40 μm.

In figure 4 a simple NO profile and history concentration may be seen (with a coarse subdivision). Inside the soma (distance $< 40\mu$m) the concentration is constant. Outside, it drops until the dendritic arborization area is reached. It then drops off gradually.

The NO field created from a single neuron may be seen in figure 6.

B. Total accumulation

After a short period of time, NO accumulates to such a level that the rate of loss (through decay and spread) equals the rate of production. The total NO accumulation after a time was assumed to be proportional to the rate of production i.e. (total accumulation) $= \kappa\times$ (production

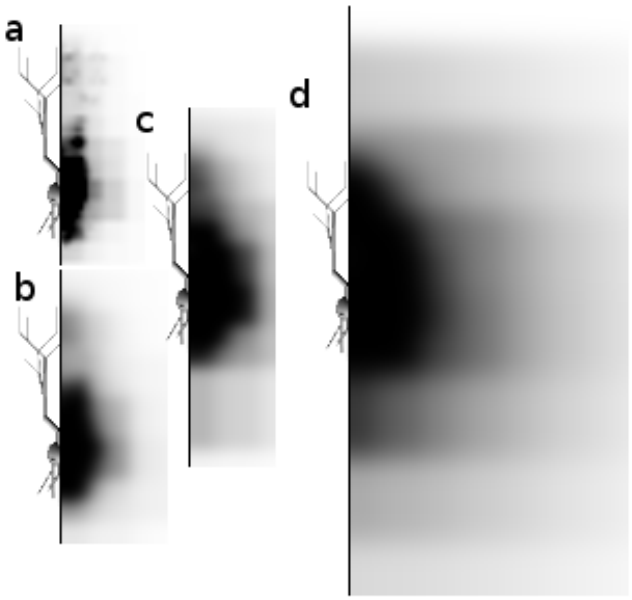

Fig. 6. NO emission from a single neuron. The neuronal structure is depicted in the left half of the images; the right half corresponds to the NO concentration mirroring the neuronal structure. The maximum darkness corresponds to a concentration of about 8.4 $\times 10^{-20}$ mol/μm^3, if a production rate of 2.1×10^{-17} is used. a) 10 ms b) 20 ms c) 50 ms d) 1000 ms and 2000 ms (both are identical).

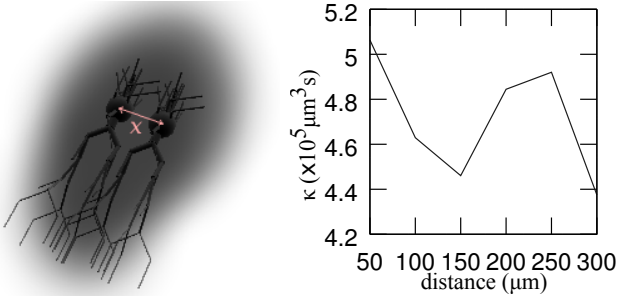

Fig. 7. Visualization of simulation of two neurons. Shown is an example case where the inter-soma distance (x) is 100 μm; and concentration is shown after 100 ms (gray shading). Right: total NO accumulation κ vs. neuron distance. After 300 μm, it becomes constant as the neurons stop 'interfering' with one another's NO production.

rate per unit volume). This assumption is valid for a linear diffusion medium.

To assess the total NO accumulation at the steady state, we sampled the total accumulation of NO in the domain at various periods of time, for a single vessel. It was found that, up to the precision of our machine (15 decimal digits) the NO concentration reached a flat plateau at 6.0 seconds. The constant of proportionality at this time was $\kappa = 2.4 \times 10^5 \mu\text{m}^3\text{s}$.

We then simulated two (identical) neurons at various distances from each other and recorded the maximum NO concentration. See figure 7.

V. Conclusion

The combined effects of two neurons can be seen in figure 8. Assuming reasonable values for nitric oxide production,

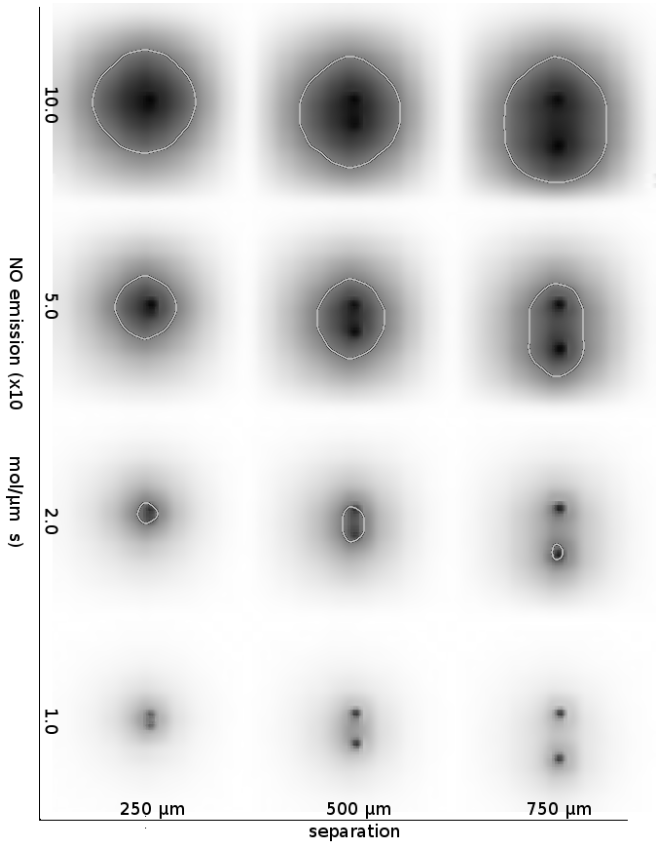

Fig. 8. Visualization of the steady-stade MLC dephosphorylation rate at various distances from the neurons using different rates for NO emission (top-down) and different values of separation between neurons (left-right). What is shown is a slice of the 3-d field at the plane perpendicular to the neuronal axes and containing both neurons. The dimensions of the area are 3.2 mm on each side, with one neuron in the center and the other a distance above it. Black is maximum dephosphorylation, white is minimum. The white ellipsoids are the isolines where the rate is half of its maximum value.

neurons have the ability to influence vasodilation at distances far from the neuron body. Given that microimaging techniques show the usual inter-neuron distance in the brain to be on the order of tens of micrometers [5], the number of vessels in an area of the order of millimeters is large. Even assuming production values at the low end of the scale (top of figure 8), many vessels are influenced.

As verified in figures 7 and 8, the addition of a second neuron to a system mainly results in a linear superposition effect, with some nonlinearities that are most visibly apparent in the values of κ. A purely linear superposition would result in a κ of $2.4 + 2.4 = 4.8 \times 10^5 \mu\mathrm{m}^3\mathrm{s}$, but what is seen is a fluctuation around that point, where the neurons sometimes destructively and constructively interfere in the total accumulation of NO. We hypothesize that these nonlinearities are due to high-concentration areas 'clumping' together causing localized areas of high NO concentration that have consequently higher decay rates.

REFERENCES

[1] DS Bredt and SH Snyder. Nitric oxide: a physiologic messenger molecule. *Annual Review of Biochemistry*, 63(1):175–195, 1994.

[2] I. Fleming and R. Busse. NO: the primary EDRF. *Journal of molecular and cellular cardiology*, 31(1):5–14, 1999.

[3] J.A. Gally, P.R. Montague, GN Reeke, and G.M. Edelman. The NO hypothesis: possible effects of a short-lived, rapidly diffusible signal in the development and function of the nervous system. *Proceedings of the National Academy of Sciences of the United States of America*, 87(9):3547, 1990.

[4] J. Garthwaite and CL Boulton. Nitric oxide signaling in the central nervous system. *Annual review of physiology*, 57(1):683–706, 1995.

[5] S. Heinzer, T. Krucker, M. Stampanoni, R. Abela, E.P. Meyer, A. Schuler, P. Schneider, and R. Muller. Hierarchical microimaging for multiscale analysis of large vascular networks. *Neuroimage*, 32(2):626–636, 2006.

[6] Christian Hölscher. Nitric oxide, the enigmatic neuronal messenger: its role in synaptic plasticity. *Trends in Neurosciences*, 20(7):298 – 303, 1997.

[7] P. Husbands, T. Smith, and N. Jakobi. Better living through chemistry: Evolving GasNets for robot control. *Connection Science*, 10(3):185–210, 1998.

[8] C. Iadecola. Regulation of the cerebral microcirculation during neural activity: is nitric oxide the missing link? *Trends in neurosciences*, 16(6):206–214, 1993.

[9] T. Malinski, Z. Taha, S. Grunfeld, S. Patton, M. Kapturczak, and P. Tomboulian. Diffusion of nitric oxide in the aorta wall monitored in situ by porphyrinic microsensors. *Biochemical and biophysical research communications*, 193(3):1076–1082, 1993.

[10] S. Nawy and C.E. Jahr. Suppression by glutamate of cGMP-activated conductance in retinal bipolar cells. 1990.

[11] RD Traub, JG Jefferys, R. Miles, MA Whittington, and K. Toth. A branching dendritic model of a rodent CA3 pyramidal neurone. *The Journal of Physiology*, 481(Pt 1):79, 1994.

[12] J. Wood and J. Garthwaite. Models of the diffusional spread of nitric oxide: implications for neural nitric oxide signalling and its pharmacological properties. *Neuropharmacology*, 33(11):1235–1244, 1994.

[13] J. Yang, J.W. Clark, R.M. Bryan, and C.S. Robertson. Mathematical modeling of the nitric oxide/cGMP pathway in the vascular smooth muscle cell. *American Journal of Physiology-Heart and Circulatory Physiology*, 289(2):H886, 2005.

[14] Yang Yong, Ning Gang-min, Gan Zhuo-hui, and Zheng Xiao-xiang. Modeling the diffusion of nitric oxide produced by neuronal cells in brain ischemia. In *Engineering in Medicine and Biology Society, 2005. IEEE-EMBS 2005. 27th Annual International Conference of the*, pages 7321 –7324, 2005.